Electronic Supplementary Material (ESI) for Lab on a Chip.

Supplementary Information

Laser particle activated cell sorting in microfluidics

Paul H. Dannenberg[1,2,3], Jisoo Kang[1], Nicola Martino[1,2], Anokhi Kashiparekh[1], Sarah Forward[1], Jiamin Wu[1,4], Andreas C. Liapis[1,2], Jie Wang[1,5], Seok-Hyun Yun[1,2,3,*]

[1]Wellman Center for Photomedicine, Massachusetts General Hospital, Boston, MA 02114, USA

[2]Harvard Medical School, Boston, MA 02115, USA

[3]Harvard-MIT Health Sciences and Technology, Massachusetts Institute of Technology, Cambridge, MA 02139, USA

[4]Department of Automation, Tsinghua University, Beijing, China

[5]College of Artificial Intelligence, Nanjing Agricultural University, Nanjing, China

*syun@hms.harvard.edu

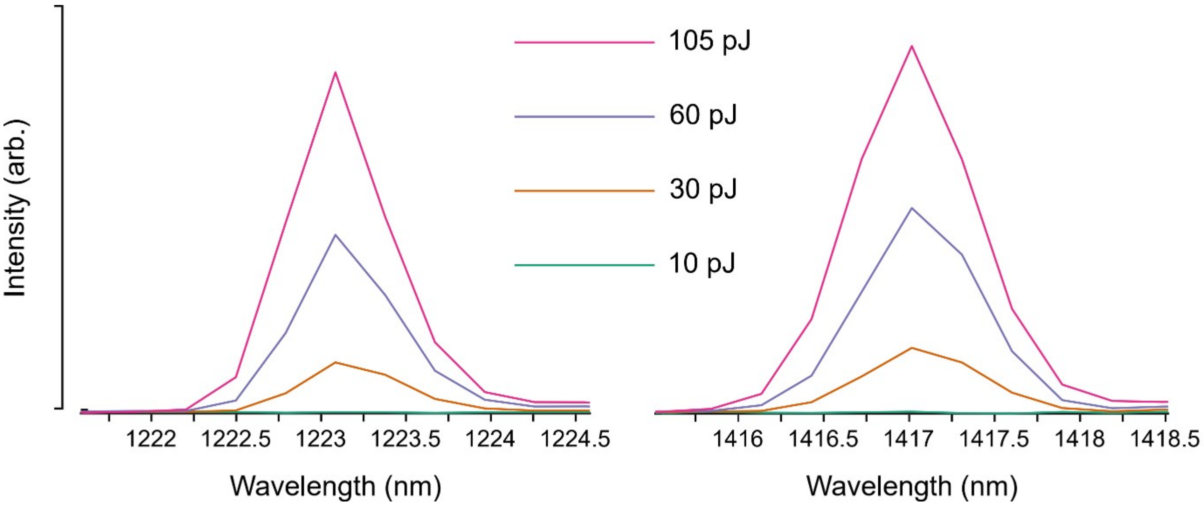

Figure S1. Lasing spectra of LPs at different pump energies. a, LP emission intensity and wavelength of two representative LPs following excitation using a 2 MHz, 10 ns pulse width laser excitation with pulse energies of 10 pJ (green), 30 pJ (orange), 60 pJ (violet), and 105 pJ (pink).

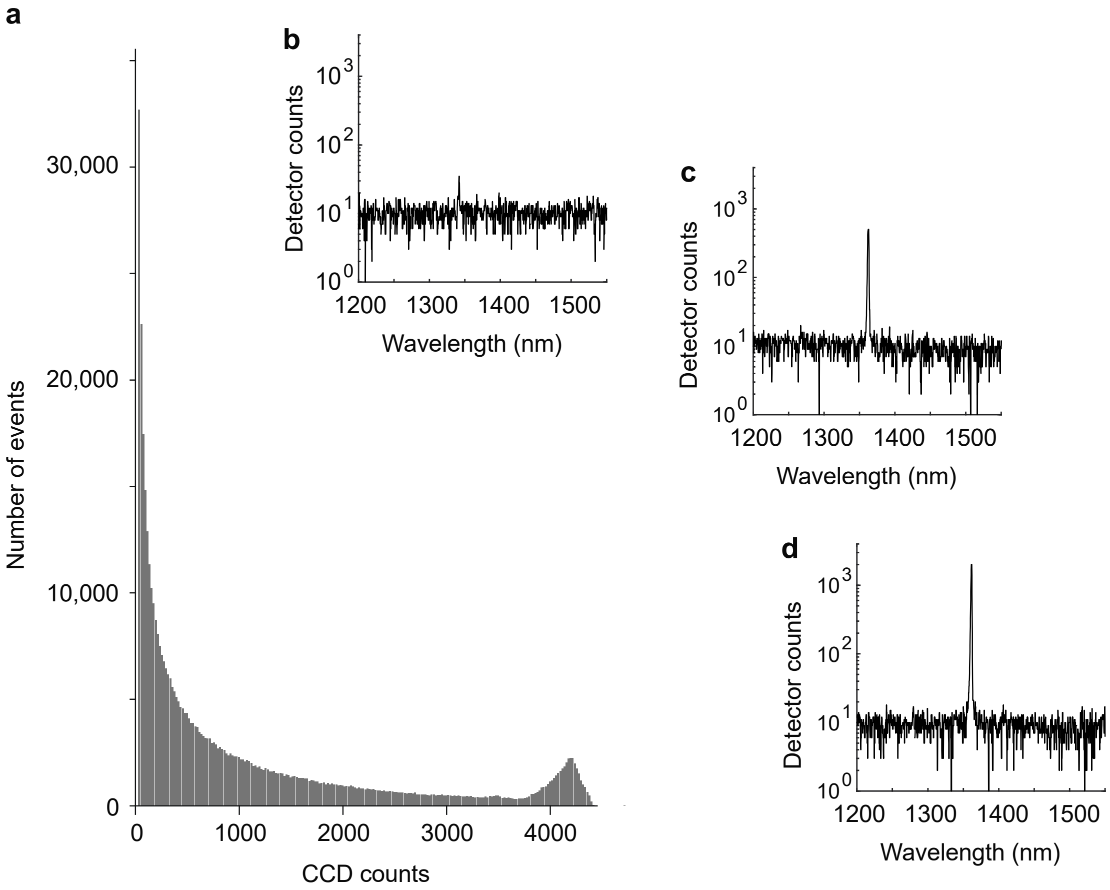

Figure S2. Lasing spectra of LPs in the flow. a, the distribution of spectral peak intensity from over 460,000 LPs (Fig. 1), recorded by the line scan camera of the spectrometer. The typical detector noise floor level is 25-30 counts. The increase in the number of events with peak counts of > 4000 is caused by saturation of the detector. **b-d**, three representative spectra with lasing peaks of 30, 500 and 2000 counts, respectively, measured during flow along the straight channel shown in Fig. 1.

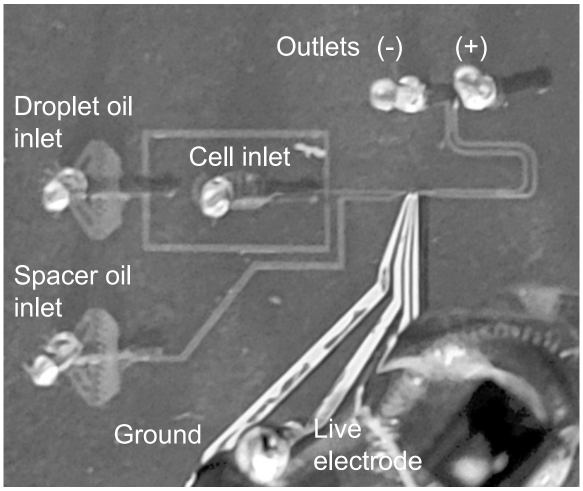

Figure S3. A photograph of the microfluidic sorting chip used in the experiment. See Fig. 2a for its schematic drawing.

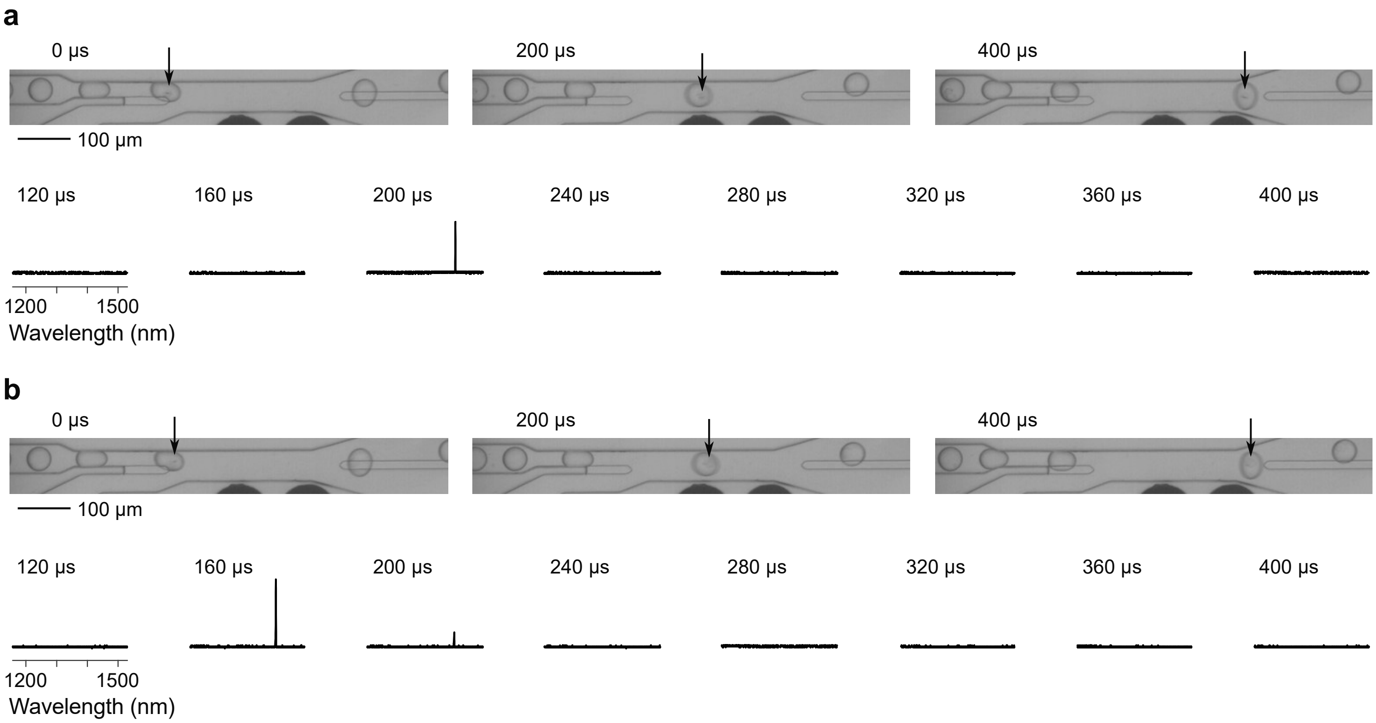

Figure S4. Real-time identification of LP emission during sorting. Bright-field images, taken at a frame rate of 5 kHz with an exposure time of 14 µs, of two LP-containing cells (arrows) within aqueous droplets as a function of time elapsed. The emission spectra were acquired at a frame rate of 25 kHz. **a**, a cell traversing the detection point resulting in a lasing peak in only a single frame. See Video 1. **b**, a different cell with its lasing peak detected in two consecutive frames. See Video 2.

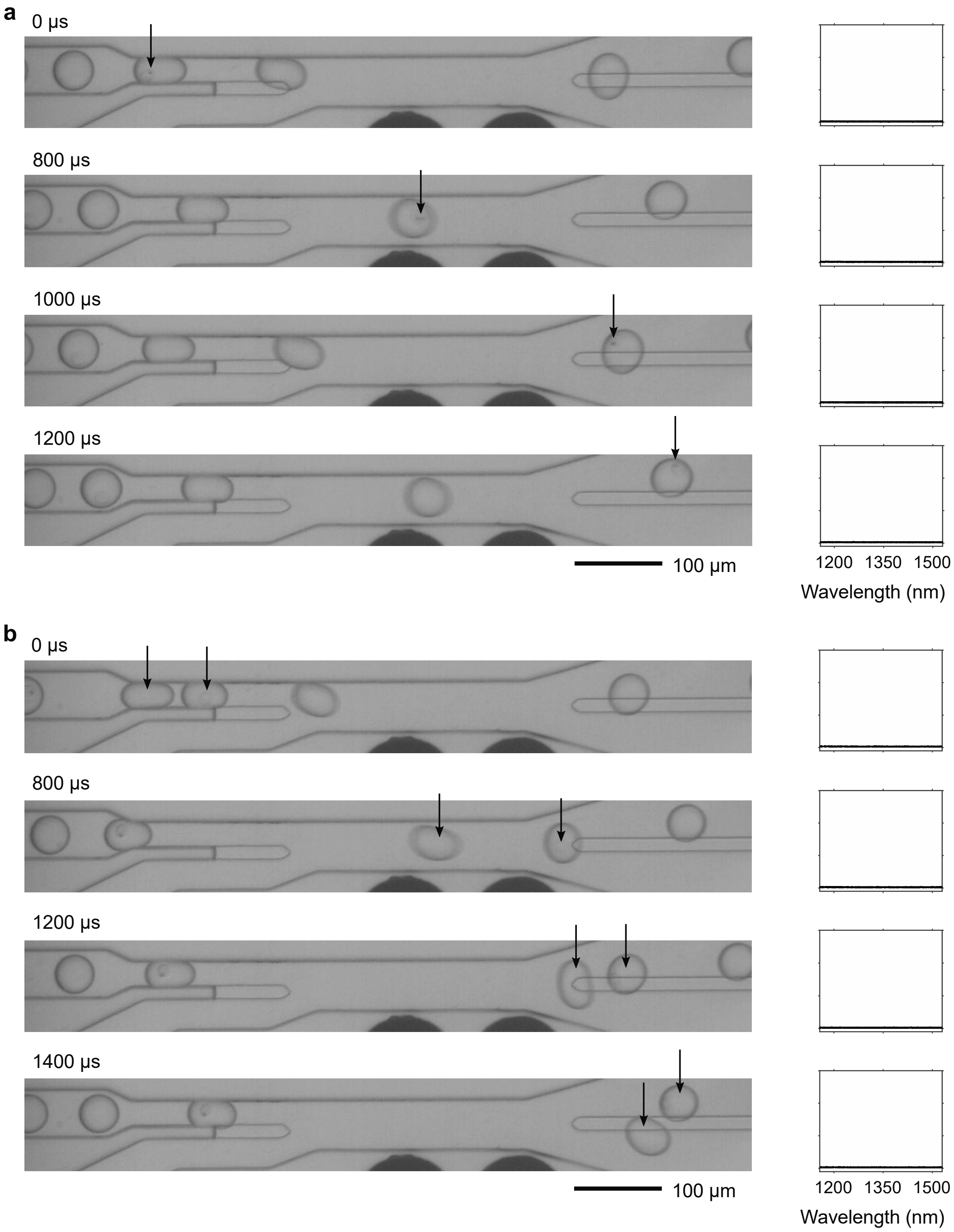
a
0 µs
800 µs
1000 µs
1200 µs
100 µm
1200
1350
1500
Wavelength (nm)
b
0 µs
800 µs
1200 µs
1400 µs
100 µm
1200
1350
1500
Wavelength (nm)

(Continued)

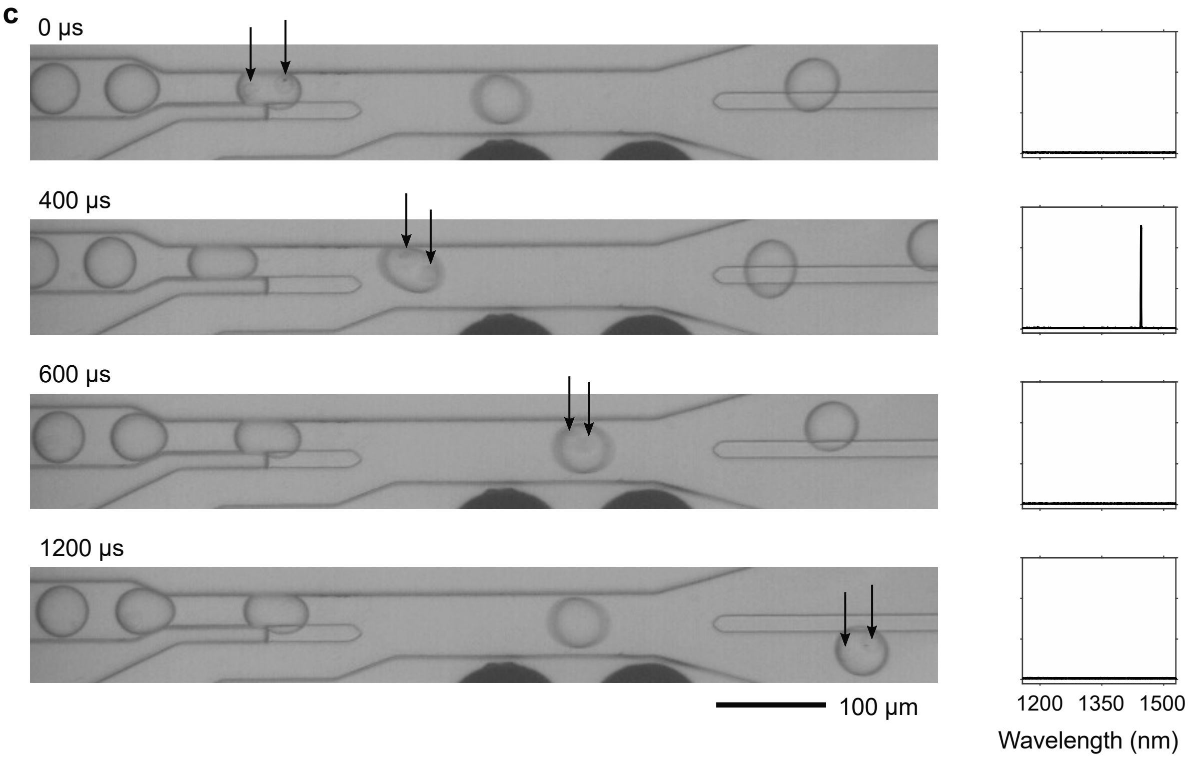

Figure S5. Three failure modes of sorting error. Bright-field images (left column) at various timepoints along with corresponding recorded spectra (right column). **a**, lasing from an intracellular LP (arrow) is not detected. The sorting mechanism is not activated, and the cell is routed to the (-) channel, generating a false negative error. See Video 3. **b**, an instability in the flow causes two droplets (arrows) to bunch closer than the normal distance. The second droplet collides with the first, causing it to be deflected towards the (+) channel without a lasing detection event. See Video 4. **c**, a single droplet contains two cells (arrows). One cell contains an LP, and the other does not. Both are deflected towards the (+) outlet. This results in one cell with a false positive error. See Video 5.

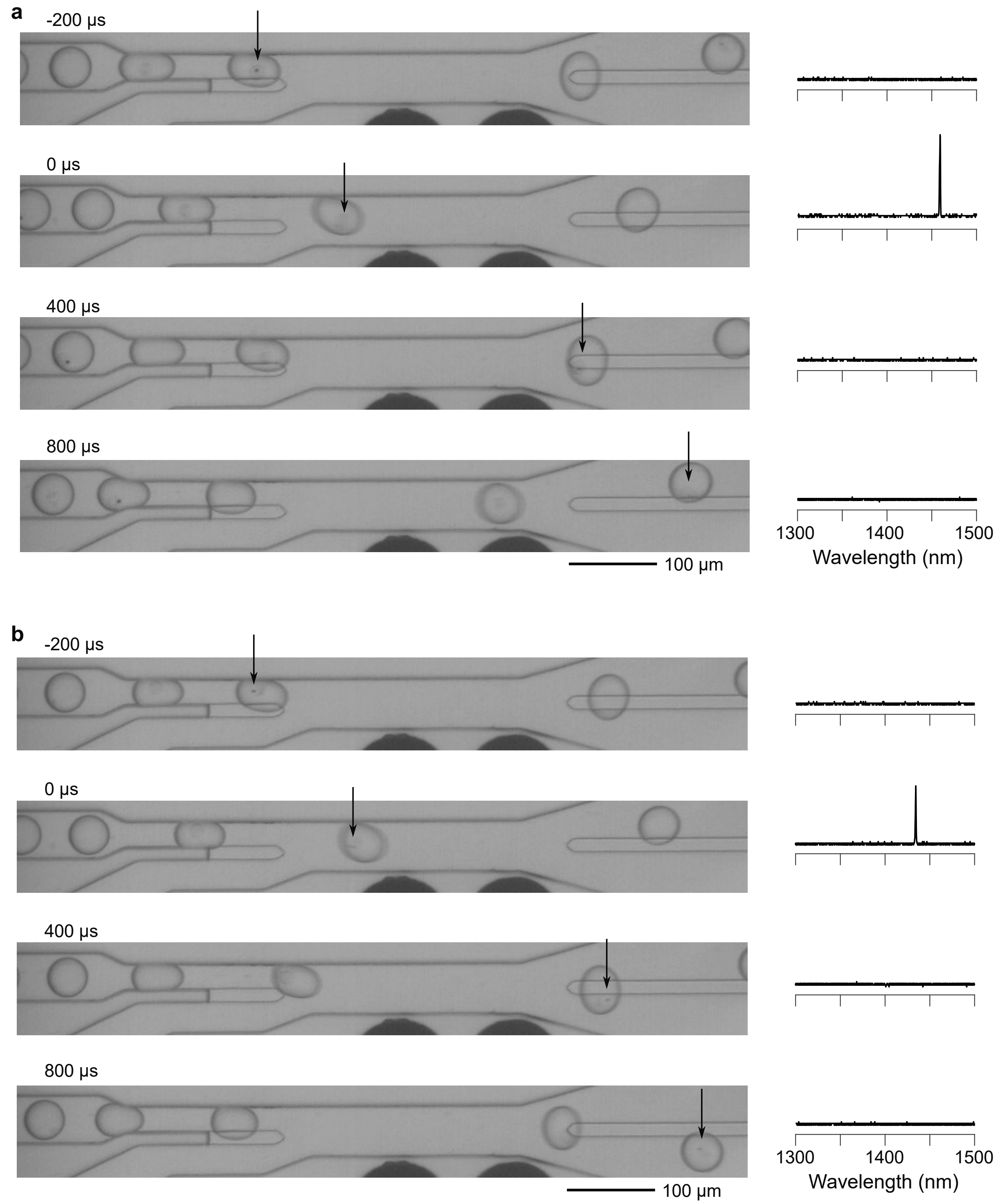

Figure S6. Wavelength-dependent sorting. Cells are sorted based on their emission wavelength with a cutoff at 1450 nm. **a**, a cell with a lasing peak > 1450 nm is directed into the (-) outlet, and **b**, a cell with ≤ 1450 nm is routed to the (+) outlet. See Videos 6 to 8.

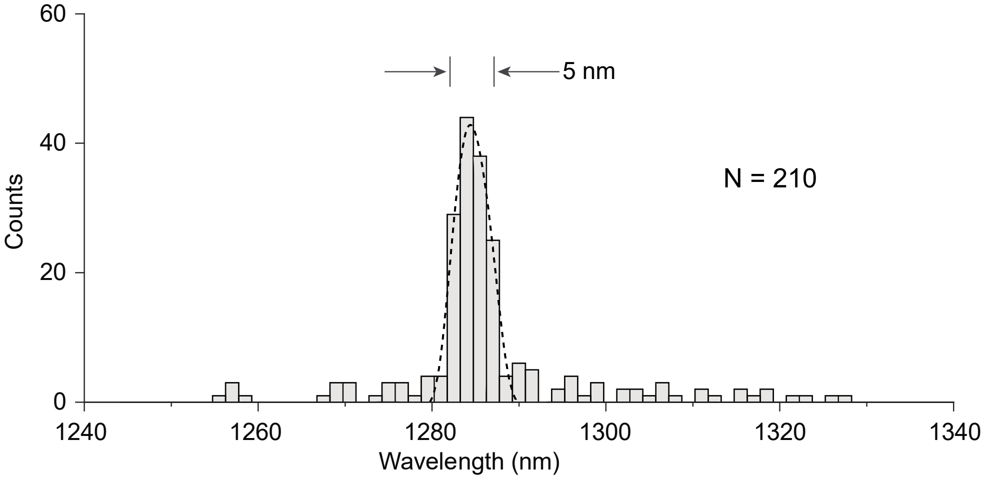

Figure S7. Wavelength distribution of LPs in the (+) outlet after bandpass sorting for 1285 +/- 2.5 nm.

Supplementary Note 1: The principle of dielectrophoresis

The derivation of a dielectrophoretic force acting on a droplet is, for completeness, given here. The same argument can also be found in Bruus (*Theoretical Microfluidics*, Oxford University Press, 2007).[1]

Droplets are sorted via the mechanism of dielectrophoresis in which a droplet of high dielectric constant ($\epsilon_2 \approx 80$) embedded in an oil of much lower dielectric constant $\epsilon_1 \ll \epsilon_2$ is attracted by a non-uniform electric field. Intuitively this attractive force occurs since the droplet is polarized by the field to a greater extent than the surrounding oil. The polarized droplet has a resultant dipole moment, which is then attracted by a non-uniform electric field, which exerts a greater attractive force on one end of the dipole than the repulsive force on the dipole's other end. A simple model is shown below, in which an electric field acts on the droplet.

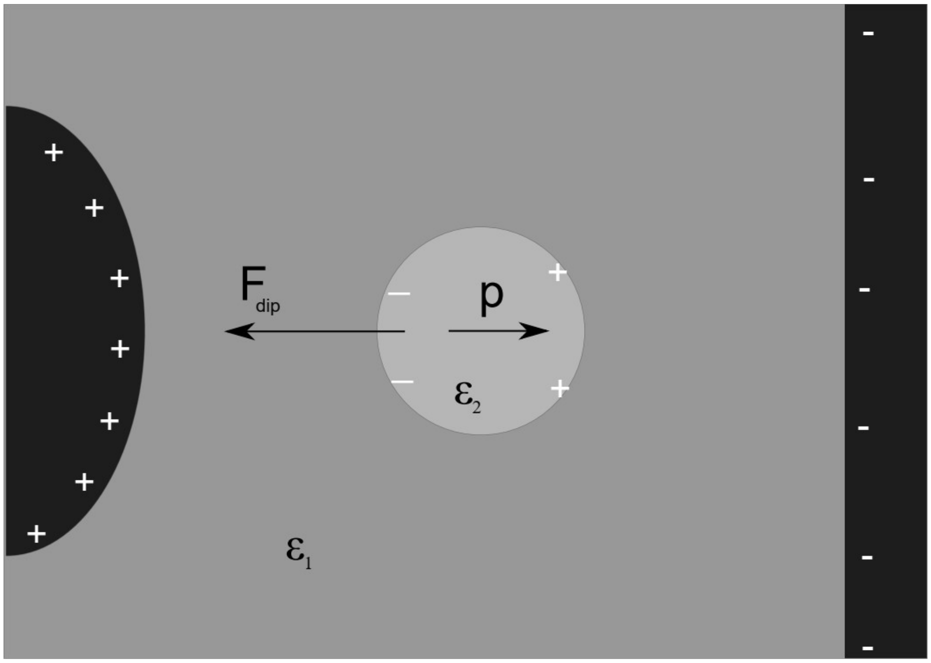

Figure S8. Dielectrophoresis. Droplet (light grey) embedded in another dielectric (grey). The electrodes (black) generate an electric field. In the case that $\epsilon_1 \ll \epsilon_2$, the polarization vector acts to the right.

Note that since the droplet is more easily polarized due to the relatively large value of ϵ_2, there is a net positive bound surface charge in the region away from the positive electrode and a net negative bound charge close to the positive electrode. Overall, there is a non-zero net polarization vector, which experiences a force in $F_{\text{dip}} = (p \cdot \nabla) E$ an electric field. To derive an expression for this force, we first start with the solvable approximate case of a droplet embedded within a uniform electric field $E = E_0 \hat{z}$ with a coordinate system whose origin is at the center of the droplet. The electrostatic potential before adding the droplet is thus

$$\phi_0(r,\theta,\varphi) = -E_0\, z = -E_0\, r\cos\theta \tag{S1}$$

where we have introduced the usual spherical coordinate system. The electrostatic potential after adding the droplet of radius a will change, since the droplet will be polarized, generating its own electric field. After the addition of the droplet, we can describe ethe electrostatic potential ϕ by

$$\phi(r,\theta,\varphi) = \begin{cases} \phi_1(r,\theta) & r > a \\ \phi_2(r,\theta) & r < a \end{cases} \tag{S2}$$

The solutions for ϕ_1 and ϕ_2 are well known and can be expressed by solving Laplace's equation $\nabla^2\phi(r) = 0$. The solutions can be expressed in spherical coordinates by a set of Legendre polynomials $\phi(r,\theta) = \sum_{l=0}^{\infty}\left(A_l r^l + B_l r^{-(l+1)}\right)P_l(\cos\theta)$ suggesting a trial solution

$$\begin{aligned} \phi_1(r,\theta) &= -E_0\, r\cos\theta + B\frac{\cos\theta}{r^2} \\ \phi_2(r,\theta) &= A\, r\cos\theta \end{aligned} \tag{S3}$$

If we consider the complete set of boundary conditions which state that $\phi_2(0,\theta)$ is finite, $\phi_1(a,\theta) = \phi_2(a,\theta)$, $\epsilon_1\frac{\partial\phi_1(a,\theta)}{\partial r} = \epsilon_2\frac{\partial\phi_2(a,\theta)}{\partial r}$, and $\lim_{r\to\infty}\phi_1(r,\theta) = -E_0\, r\cos\theta$, we can solve for the constants A and B resulting in

$$\phi(r,\theta,\varphi) = \begin{cases} -E_0\, r\cos\theta + \frac{\epsilon_2-\epsilon_1}{\epsilon_2+2\epsilon_1}a^3E_0\frac{\cos\theta}{r^2} = \phi_0(r) + \phi_{\text{dip}}(r) & r > a \\ \frac{-3\epsilon_1}{\epsilon_2+2\epsilon_1}E_0\, r\cos\theta = \frac{-3\epsilon_1}{\epsilon_2+2\epsilon_1}\phi_0(r) & r < a \end{cases} \tag{S4}$$

Here we note that the potential outside the sphere is simply the unperturbed potential ϕ_0 along with a second term that resembles a the potential due to a dipole. Since a dipole has a potential $\phi_{\text{dip}}(r) = \frac{1}{4\pi\epsilon}\frac{p\cdot r}{r^3} = \frac{1}{4\pi\epsilon}\frac{p\cos\theta}{r^2}$, we see that the situation is analogous to a perfect dipole with moment

$$p = 4\pi\epsilon_1\frac{\epsilon_2-\epsilon_1}{\epsilon_2+2\epsilon_1}a^3E_0 \tag{S5}$$

Situated at the origin. This dipole will be subject to a force in the presence of a non-uniform electric field. An approximate solution can be calculated if we assume that significant variations in the electric field take place over a distance much larger than the characteristic length scale a of the droplet. In this case, we can assume the electric field is roughly uniform across the droplet and so $E_0(r) \approx E_0(0)$, the electric field at the center of the droplet. In this case, it is straightforward to calculate the force exerted on the dipole-approximated-droplet.

$$\begin{aligned} F_{\text{dip}}(r_0) &\approx \left(p(r_0)\cdot\nabla\right) E_0(0) \\ &= 4\pi\epsilon_1 \frac{\epsilon_2-\epsilon_1}{\epsilon_2+2\epsilon_1} a^3 \left(E_0(0)\cdot\nabla\right) E_0(0) \\ &= 2\pi\epsilon_1 \frac{\epsilon_2-\epsilon_1}{\epsilon_2+2\epsilon_1} a^3 \,\nabla\left(E_0(0)^2\right) \end{aligned} \tag{S6}$$

where in the last step we have used the identity $\nabla(E^2) = 2\,(E\cdot\nabla)\,E$ for a field E with zero curl. Note that while the direction of the dipole is dependent on the direction of the electric field, the force is not. Instead, it is dependent on the field's square magnitude. Intuitively the arises because the polarization of the droplet has been assumed to be linearly on the field, while the force introduces a second contribution from the electric field. Therefore, the total force is dependent not on the direction of the electric field but on its magnitude and the relative sizes of ϵ_1 and ϵ_2. Indeed, force can be made to be repulsive if the dielectric constant of the droplet is lower than that of the surrounding fluid. Because the direction of the electric field has little effect on the generation of force, an AC current is usually preferred in dielectrophoretic sorting since it additionally prevents the buildup of charged layers around the electrodes which would screen their effects.

Supplementary Note 2: Analysis of sorting accuracy

Wed define the following parameters:

s as the sensitivity. This is the probability that a positive cell (for example, a cell containing 1 or more LPs or a cell containing an LP emitting within a defined spectral window) will be actively sorted to the (+) outlet.

s_p as the specificity. This is the probability that a negative cell (for example, a cell containing no LPs or a cell not containing an LP emitting within a defined spectral window) will be passively sorted to the (-) outlet.

p_+ as the fraction of cells identified from the (+) outlet that were correctly sorted into this outlet. This is also known as the positive predictive value.

p_- as the fraction of cells identified from the (-) outlet that were correctly sorted into this outlet. This is known as the negative predictive value.

P_+ as the fraction of cells that flow into the sorting junction that are positive cells.

Then, we can write

$$p_+ = \frac{s P_+}{s P_+ + (1 - s_p)(1 - P_+)} \tag{S.1}$$

$$p_- = \frac{s_p (1 - P_+)}{(1 - s) P_+ + s_p(1 - P_+)} \tag{S.2}$$

Rearranging these expressions for s and s_p gives

$$s = \frac{P_+ p_+ - p_+ + p_- p_+}{P_+ p_- - P_+ + P_+ p_+} \tag{S.3}$$

$$s_p = -\frac{P_+ p_- - p_- p_+}{P_+ + p_- + p_+ - P_+ p_- - P_+ p_+ - 1} \tag{S.4}$$

In the scenario of sorting between cells with and without LPs, we calculate s and s_p based on the values $p_+ = 0.94$, $p_- = 0.99$, and $P_+ = 0.70$, which can be obtained from the experimental data shown in Fig. 3.

Supplementary Note 3: Analysis of wavelength-based sorting accuracy

In the case of wavelength-based LACS, the values for s and s_p can be deduced by looking at the cumulative distribution of emission wavelengths. We define the (+) outlet as the one in which the cells were desired to be tagged with LPs emitting within the ± 2.5 nm sorting window. Figure S9 reveals the fraction $p_+ = 0.58$ of the LPs that emitted within this spectral window. The (-) outlet collected the passive flow of cells. The graph reveals that the fraction $p_- = 0.98$ of LPs do not emit within the sorting window. The fraction of LPs emitting within the sorting window of cells before they are sorted provides a value of $P_+ = 0.08$. Using these values with Eq. S.3 and Eq. S.4 gives $s = 0.81$, $s_p = 0.95$.

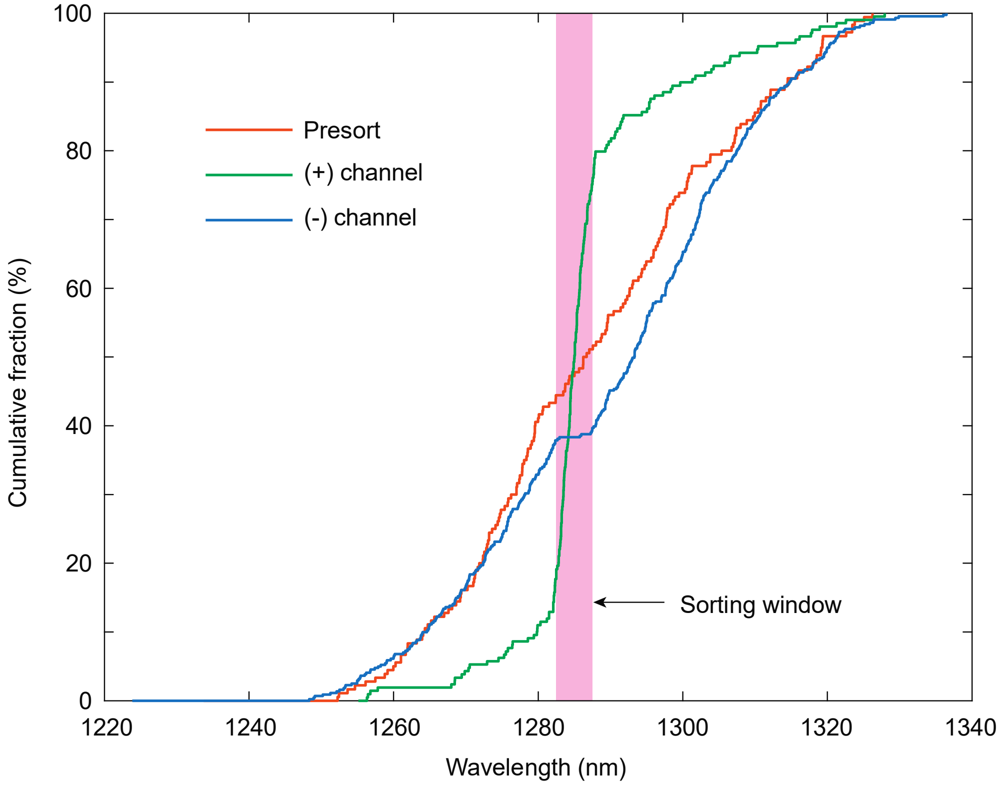

Figure S9. Cumulative distribution of LP wavelengths before and after LACS. The red curve shows the cumulative distribution of 181 measured cells before sorting. The blue curve shows the cumulative distribution of 442 cells that were collected from the (-) outlet. The green curve shows the lasing wavelength distribution of 210 measured LPs collected from the (+) outlet.

Supplementary Note 4: Temperature dependence of LP resonance wavelength

In one of the simplest models of a disk-shaped LP, the resonance wavelength λ_m of integer mode m can be roughly expressed as $\lambda_m = \frac{2\pi nR}{m}$ where n is the LP refractive index, and R is its radius. If we assume that the wavelength dependence is a function of temperature T only due to temperature-based variations in its refractive index and radius, we can express this variation as

$$\frac{d\lambda_m}{dT} = \frac{2\pi}{m}\left(\frac{dn}{dT}R + n\frac{dR}{dT}\right) = \frac{2\pi R}{m}\left(\frac{dn}{dT} + n\alpha\right)$$

where we have introduced the linear thermal expansion coefficient α. From the literature, typical values for a III-V semiconductor are $\frac{dn}{dT} \approx 2 \times 10^{-4}K^{-1}$ and $\alpha \approx 5 \times 10^{-6}K^{-1}$.[2,3] For the lasing mode $m = 16$ (which corresponds to a resonance wavelength $\lambda_{16} = 1355$ nm for $R = 1$ µm and $n = 3.45$) the change in wavelength per Kelvin is therefore $\frac{d\lambda}{dT} \approx 0.085$ nm/K.

Description of Supplementary Videos

- Video 1: An exemplary cell sorted into the (+) channel (Fig. S4a).
- Video 2: Another cell sorted (Fig. S4b).
- Video 3: Failure mode: A missed detection event (Fig. S5a).
- Video 4: Failure mode: Flow instability resulting in droplet collision (Fig. S5b).
- Video 5: Failure mode: Two cells in a single droplet (Fig. S5c).
- Video 6: Example of short-wavelength sorting.
- Video 7: Example of short-wavelength sorting.
- Video 8: Example of short-wavelength sorting

References

1 H. Bruus, *Theoretical Microfluidics*, Oxford University Press, 2007.

2 M. Levinshtein, S. Rumyantsev and M. Shur, , DOI:10.1142/2046-VOL1.

3 A. Waqas, D. Melati, Z. Mushtaq, B. S. Chowdhry and A. Melloni, *Wirel. Pers. Commun.*, 2017, **95**, 607–615.